Supplementary Material

Supplementary Figures

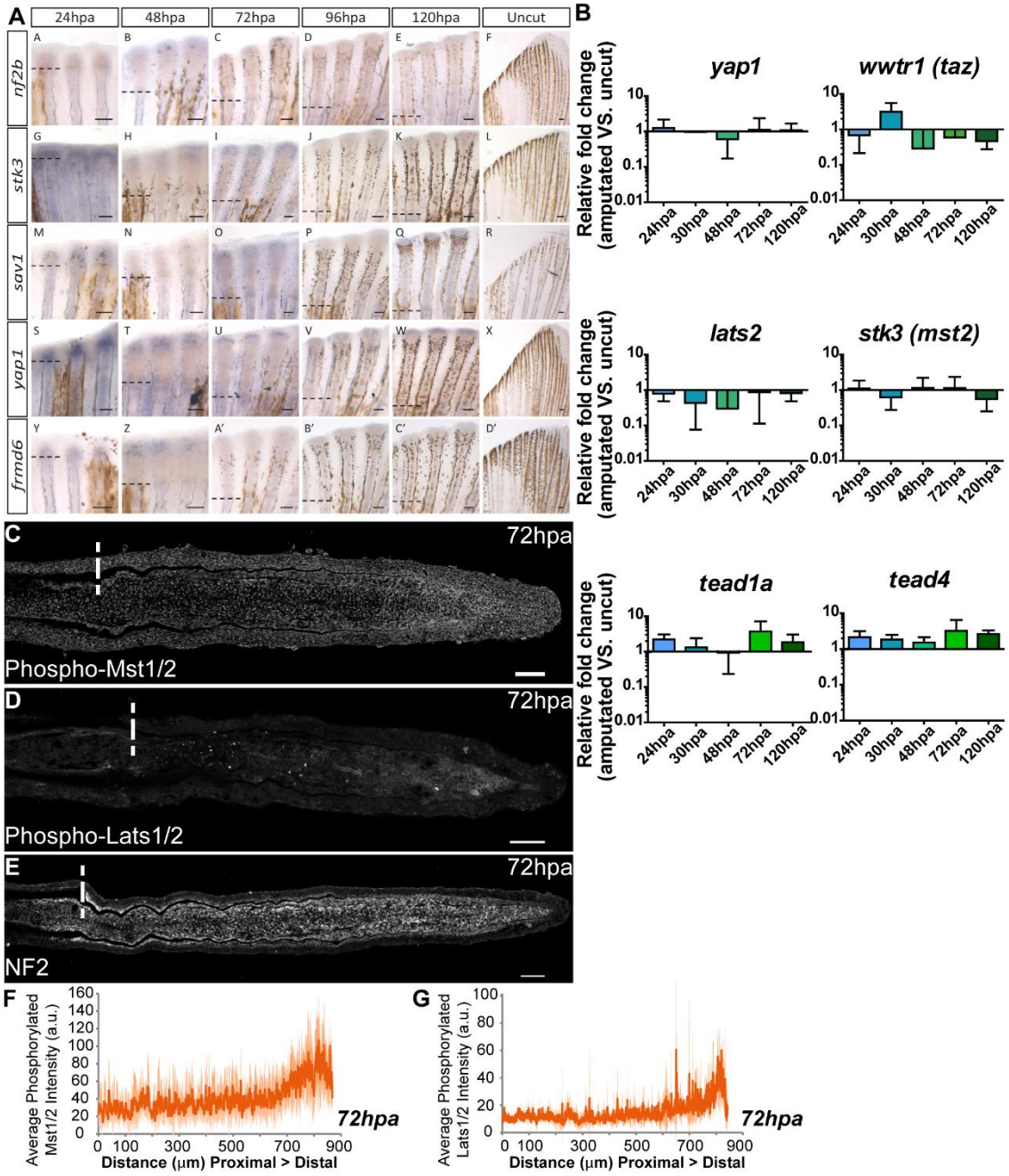

Fig. S1. Hippo pathway components are present during zebrafish caudal fin regeneration. Related to Fig 1. A Representative *in situ* hybridizations for *nf2b*, *stk3 (mst2)*, *sav1*, *yap1* and *frmd6 (expanded)* at 24 hpa, 48hpa, 72 hpa, 96 hpa, 120 hpa and uncut fins. n=3 fins per

condition. Scale bars correspond to 100µm. **B** qPCR determination of *yap1*, *wwtr1 (taz), lats2, stk3 (mst2), tead1a* and *tead4* relative expression levels during several regenerative stages (24 hpa, 30 hpa, 48 hpa, 72 hpa and 120 hpa) versus uncut controls. Logarithmic scale, base 10. **C-E** Representative immunofluorescence images against phosphorylated Mst 1/2 **(C)**, phosphorylated Lats 1/2 **(D)** and total NF2 **(E)** in 72 hpa blastemas. **F-G** Quantification of average phospho-Mst 1/2 **(F)** and phospho-Lats 1/2 **(G)** intensity (in arbitrary units, a.u.) in mesenchymal cells along the PD axis (µm) of blastemas at 72 hpa. n=5 sections, 3 fish per condition. Shadows indicate the standard deviation of the mean for each curve. For all measurements, areas from the medial blastema were considered. Dashed lines indicate amputation plane. Scale bars correspond to 50µm.

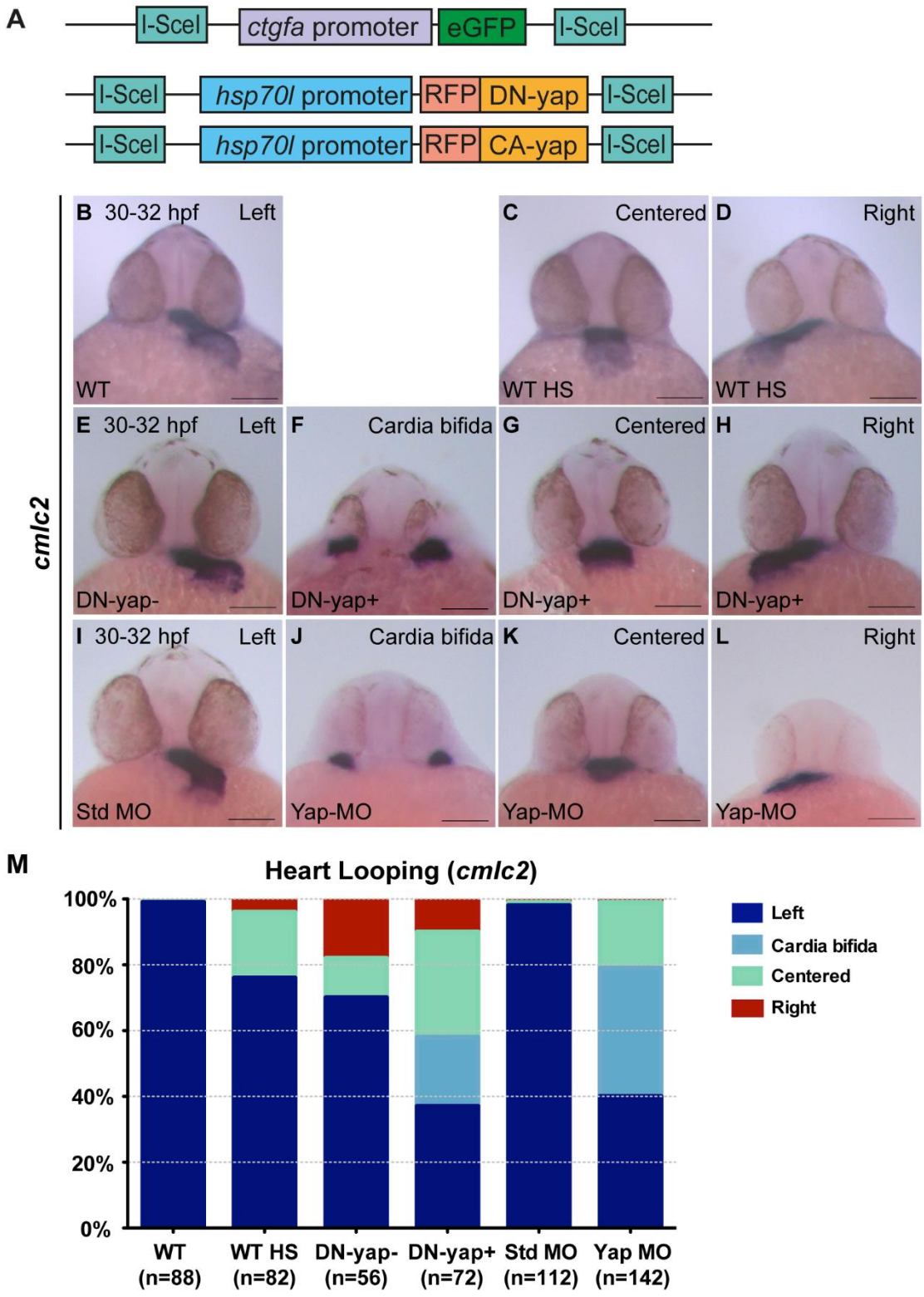

Fig. S2. DN-Yap transgenic line regulates cardiac precursor cell migration. Related to Fig 2. A Schematics of the constructs of the transgenics used in this study. Note that CA-yap transgenics have mutated the five *yap1* consensus motifs HxRxxS recognized by Lats 1/2,

having the Serines substituted by Alanines, not allowing Yap to be inactivated through phosphorylation (Zhao et al., 2007). In DN-yap transgenics, a truncated form of CA-yap was used, in which the transcriptional activation domain was removed, but its Tead binding domain was left intact, allowing Yap to bind to its DNA partner but not activate its targets (Zhao et al., 2007). **B-M** Zebrafish embryos with 30-32 hpf examined for cardiac jogging by *in situ* hybridization for *cmlc2*. **B-D** WT embryos with normal left-sided heart jogging (99%) (**B**) and few centered hearts (1%) (not shown). WT embryos given a heat-shock (hs) at 16 cells stage develop centered (20%) (**C**) and right-sided hearts (4%) (**D**), consequence of the hs itself. **E-H** A hs was given to DN-yap siblings (DN-yap-) at 16 cells stage, with the majority of embryos developing left-sided hearts (70%) (**E**), centered (12%) and right-sided (18%) hearts, the latter being a consequence of the hs itself (not shown). DN-yap positive (DN-yap+) transgenic embryos were activated at 16 cells stage with a hs and develop cardia bífida (21%) (**F**), a characteristic phenotype of loss of Yap (Fukui et al., 2014; Miesfeld and Link, 2014). They also develop centered (32%) (**G**), right (10%) (**H**) and left-sided hearts (37%) (not shown). **I-L** Standard-MO (6 ng) WT injected embryos develop mainly left-sided hearts (98%) (**I**), with few developing centered (1%) and right-sided (1%) hearts (not shown). Yap-MO (6 ng) WT injected embryos develop cardia bífida (39%) as previously shown (**J**) (Fukui et al., 2014; Miesfeld and Link, 2014). They also develop centered (20%) (**K**), right (1%) (**L**) and left-sided hearts (40%) (not shown). **M** Percentage of embryos with different phenotypes for heart jogging. Total number of embryos is shown in the bottom of each column. All scale bars are 100μm.

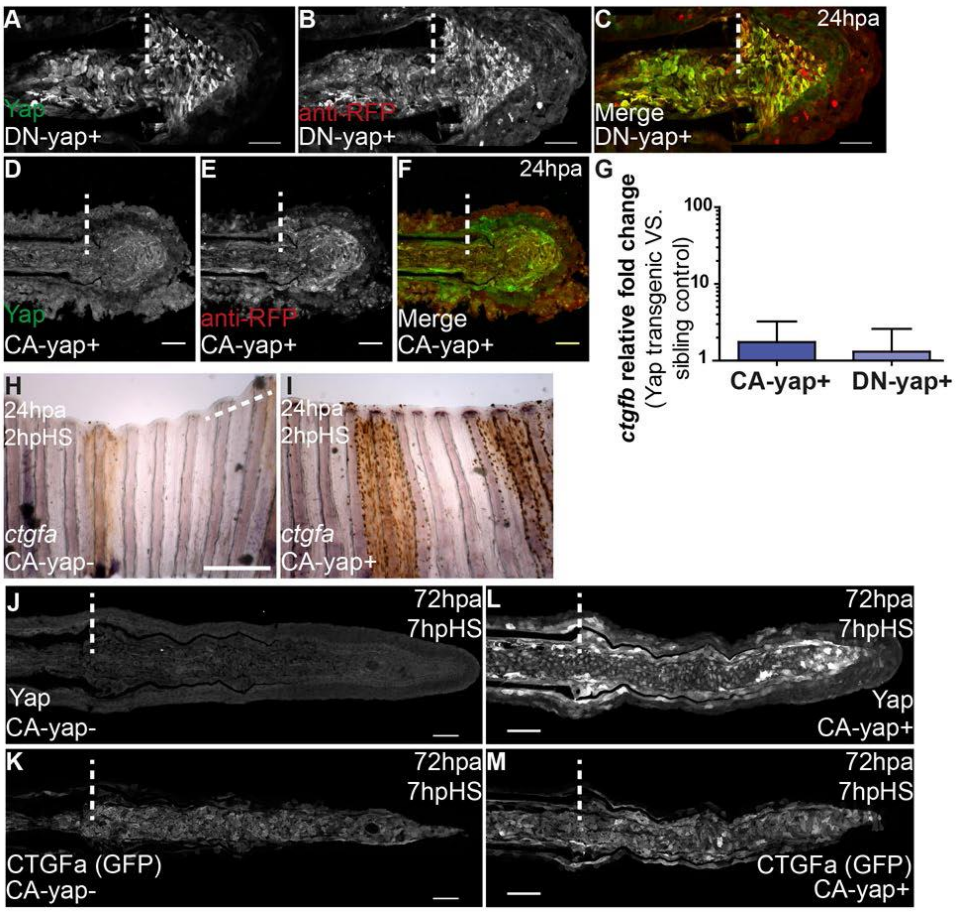

Fig. S3 *ctgfa* is conserved as a direct transcriptional target of Yap in zebrafish. Related to Figs 2 and 3. A-F Representative immunostainings with anti-Yap and anti-RFP in 24 hpa longitudinal sections of CA-yap and DN-Yap positive transgenics, upon heat-shock. **A-C** DN-Yap+; **D-F** CA-Yap+. Note that for further experiments anti-Yap was used instead of anti-RFP due to clearer intracellular labeling. **G** qPCR determination of *ctgfb* relative expression levels in CA-yap and DN-yap positive transgenics versus respective sibling controls, upon single heat-shock at 72 hpa. Logarithmic scale, base 10. **H-I** Representative *in situ* hybridization for *ctgfa* in 24 hpa fins of CA-yap sibling control **(H)** and CA-yap+ fish **(I)**. Fins were collected at 2 hpHS. n=3 fins per condition. Scale bars correspond to 500µm. **J-M** Representative immunostainings with anti-Yap and anti-GFP in 72 hpa longitudinal sections of *ctgfa*:eGFP; CA-yap double transgenics, fins were fixed at 7 hpHS. **J,K** CA-yap sibling control; **L,M** CA-yap+. Note that due to high Yap levels in L, normal settings in acquisition of images in J, L had to be decreased to avoid image saturation. n=9 sections, 3 fish per condition. Scale bars correspond to 50µm. Dashed lines indicate amputation plane.

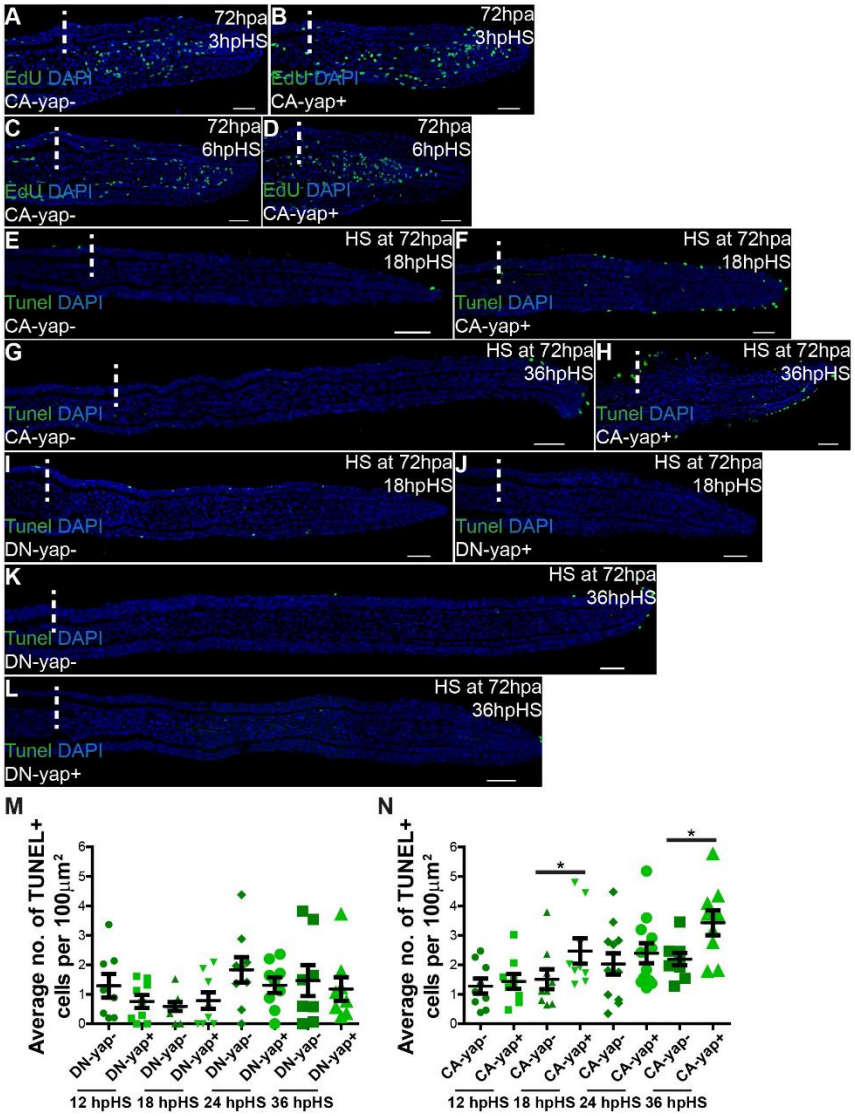

Fig. S4 Cell death occurs after the proliferative boost in CA-Yap transgenics but not in DN-Yap transgenics. A-D Representative immunofluorescence with EdU in 72 hpa longitudinal sections of CA-yap sibling controls **(A)** and CA-yap positive fish **(B)** at 3 hours post single heat-shock (hpHS); CA-yap sibling controls **(C)** and CA-yap positive fish **(D)** at 6 hpHS. Representative immunofluorescence with Tunel in 90 and 108 hpa longitudinal sections of CA-yap sibling controls (**E,G**), CA-yap positive (**F,H**), DN-yap sibling controls (**I,K**) and DN-yap positive transgenics (**J,L**). Scale bars correspond to 50µm. **M-N** Quantification of average Tunel positive cells occurring per 100µm^2 in DN-yap and siblings (**M**) and CA-yap and siblings (**N**), at different times post amputation, after a single heat-shock at 72 hpa. *P value<0.05, two tailed, non-parametric Mann-Whitney test. n=9 sections, 3 fish per condition. Dashed lines indicate amputation plane.

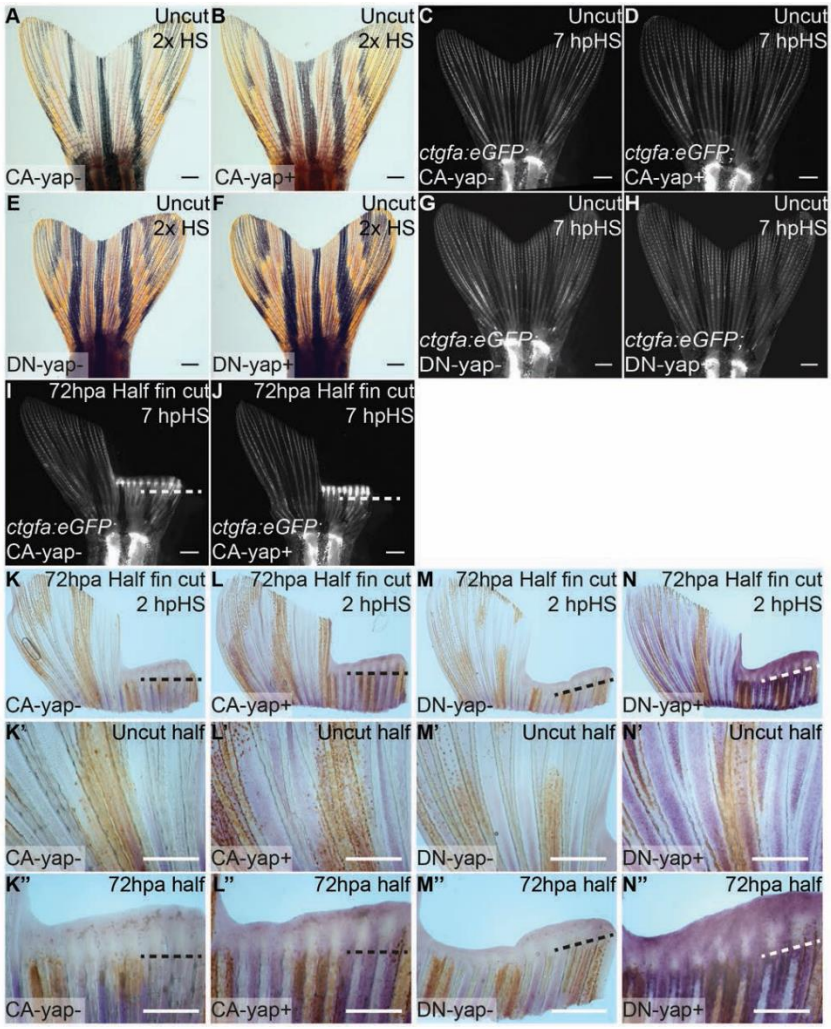

Fig. S5. Yap is not activated in a homeostatic context. A-B, E-F Representative brightfield images of uninjured CA-yap/DN-yap transgenics upon heat-shock in 2 consecutive days, phenotypes were accessed the next day. **A** CA-yap control; **B** CA-yap+; **E** DN-yap control; **F** DN-yap+. **C-D, G-H, I-J** Representative *ctgfa* expression in double transgenics *ctgfa*:eGFP; CA-yap/DN-yap and siblings upon heat-shock in uncut or 72 hpa half amputated fin animals, at 7 hpHS. **C** CA-yap control; **D** CA-yap+; **G** DN-yap control; **H** DN-yap+; **I** CA-yap control; **J** CA-yap+. n=5 fish/ condition. **K-N** Representative *in situ* hybridizations for *yap1* in 72 hpa half amputated fins of CA-yap control **(K)**, CA-yap+ **(L)**, DN-yap control **(M)**, DN-yap+ **(N)**. Corresponding zooms of uncut half **(K'-N')**, 72 hpa regenerate half **(K''-N'')** of *in situs* shown in K-N, highlighting *yap1* differences in CA-yap/DN-yap transgenics versus siblings. Fins were collected at 2 hpHS. n=3 fins/condition. Scale bars=500µm. Dashed lines indicate amputation plane.

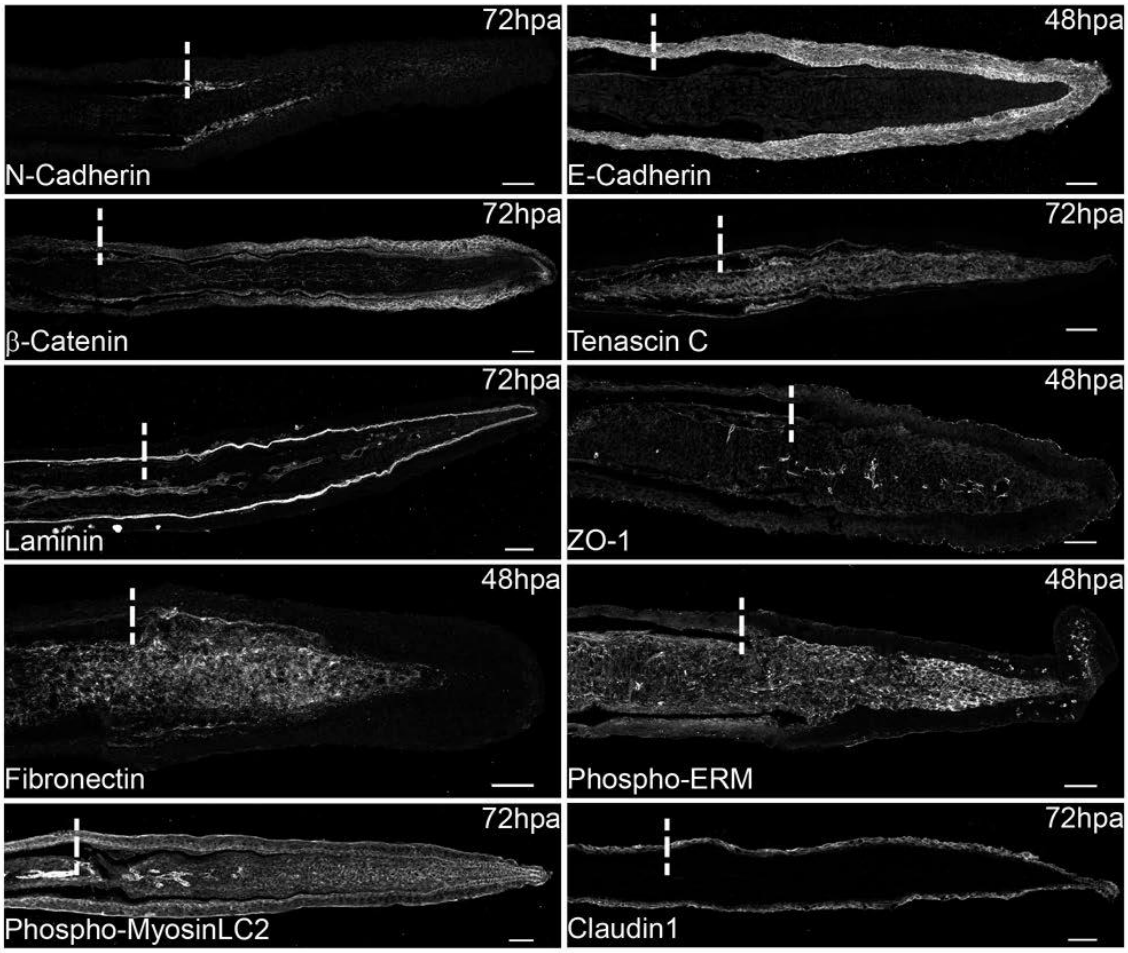

Fig. S6. Novel adhesion and cytoskeleton proteins expressed in the regenerating blastema. Related to Fig 4. Representative immunostainings of positive hits found in the adhesion and cytoskeleton related screen performed in formed blastemas (48 and 72 hpa longitudinal sections). n=3 sections per condition. Dashed lines indicate amputation plane. Scale bars correspond to 50µm.

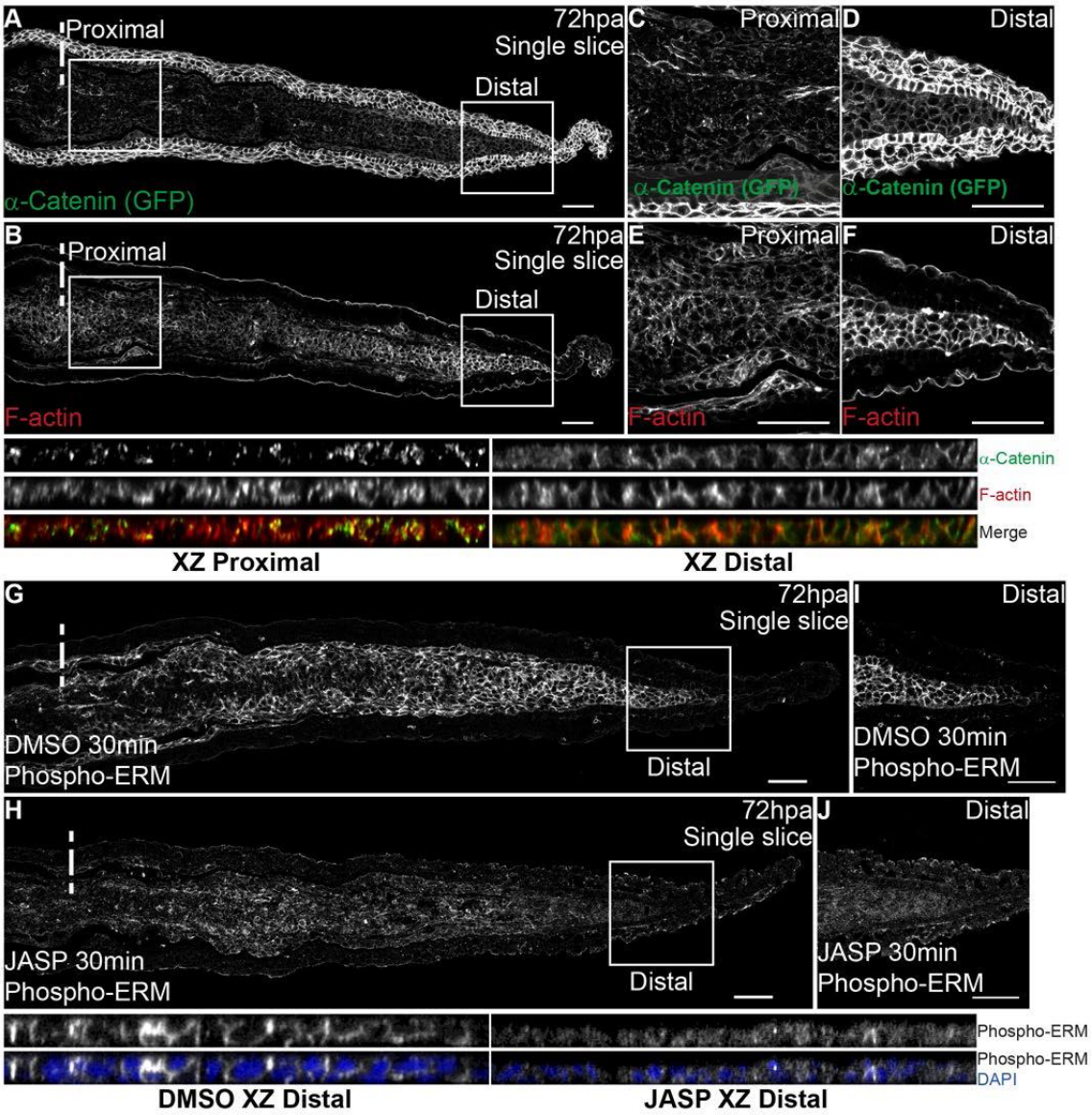

Fig. S7. α-Catenin and F-actin partially co-localize in the regenerating blastema. Related to Fig 6. A,B Representative immunofluorescence with anti-GFP and phalloidin (F-actin) in 72 hpa longitudinal sections of α-Catenin transgenics. **A** Representative single frame of α-Catenin; **B** Corresponding single frame of F-actin. **C-F** Corresponding zoomed areas represented by squares in A-B. Proximal **(C)** and distal **(D)** zoomed images from A showing the differential α-Catenin expression along the PD axis. Corresponding proximal **(E)** and distal **(F)** zoomed images from B showing the differential F-actin expression along the PD axis. Single color and merged XZ projections of proximal blastema images C,E and distal blastema images D,F are shown below the corresponding panel to highlight intracellular localization. n=9 sections, 3 fish.

G-H Representative immunofluorescence with anti-Phospho-ERM (representing F-actin) in 72 hpa longitudinal sections of animals injected with Jasplakinolide (JASP) and respective DMSO controls. Phospho-ERM expression in DMSO **(G)** and JASP **(H)** animals. **I-J** Zoomed areas represented by squares in G-H, showing Phospho-ERM expression in the distal blastema of DMSO **(I)** and JASP **(J)** animals. Corresponding XZ projections of distal blastema images I-J are shown to highlight intracellular localization in both situations; single color images showing Phospho-ERM expression and merged with DAPI. Intraperitoneal injections were performed in 72 hpa animals, 30 minutes pre-fixation of the caudal fins. n=8 sections, 4 fish per condition. Dashed lines indicate amputation plane. Scale bars correspond to 50μm.

Supplementary Materials and Methods

Transgenic line generation

The transgenic lines used were: GT(ctnna-Citrine)^{ct3a} (Žigman et al., 2010), Tg(EF1α:mAG-zGem(1/100))^{rw0410h} (Sugiyama et al., 2009). These lines were kindly provided by Mihaela Zigman and Atsushi Miyawaki. To create the *ctgfa*:eGFP reporter line, a pBSII-SK+ vector containing a 3.0Kbp upstream promoter fragment of *ctgfa*, flanked with *I-SceI* sites, was coinjected with *I-SceI* meganuclease (Roche), as published (Soroldoni et al., 2009). This construct was kindly provided by Dr. Jyh-Yih Chen and the original promoter sequence has been published by his laboratory (Chiou et al., 2006). Transgenic animals were selected starting at 1 day post fertilization (dpf) by eGFP fluorescence along the body.

To generate hsp70:RFP-CA-Yap, the constitutively active *yap1* sequence (CA-Yap) was constructed by sequentially point mutating five Serines to Alanines (S21A, S69A, S87A, S119A, S335A) with the following primers: FWD 5'-GTTCGGGGA GACGCTGAGACCGATCTGGAG-3'; REV 5'-CTCCAGATCGGTCTCAGCGTCTCC CCGAAC-3' (for S21A); FWD 5'-CAGACAAGCCGCTACAGATGCAGGTAC-3'; REV 5'-GTACCTGCATCTGTAGCGGCTTGTCTG-3' (for S69A); FWD 5'-CACGTC CGGGCACACGCTTCACCTGCCTCC-3'; REV 5'-GGAGGCAGGTGAAGCGTGTG CCCGGACGTG-3' (for S87A); FWD 5'-CTCCGCCAGTCCGCTTACGAGATACCTG-3'; REV 5'-CAGGTATCTCGTAAGCGGACTGGCGGAG-3' (for S119A); FWD 5'-TCTAGA GACGAGGCTACAGACAGTGGCCTG-3'; FWD 5'-CAGGCCACTGTCTGTAGCCTCG TCTCTAGA-3' (for S335A) (Zhao et al., 2007). The resultant CA-Yap was cloned downstream of monomeric RFP in a pcDNA3 vector with XhoI/NotI sites. The RFP-CA-Yap cassette was released and subcloned downstream of a zebrafish hsp70 promoter. To construct hsp70:RFP-DN-Yap, the dominant negative *yap1* sequence (DN-yap), was cloned by amplifying a fragment (nt 4-741) from CA-Yap and subcloned downstream of monomeric RFP in a pcDNA3 vector with XhoI/NotI sties. The RFP-DN-Yap cassette was released and subcloned downstream of the zebrafish hsp70 promoter. The final hsp70:RFP-CA-Yap and hsp70:RFP-DN-Yap constructs,

flanked with *I-SceI* sites, were co-injected with *I-SceI* meganuclease as above. Embryos were selected starting at 2 dpf by RFP fluorescence in the lens, due to endogenous hsp70 promoter activity (Lee et al., 2005). Transgenic founders were selected by examining red fluorescence in the lens in the resulting progeny. Induction of RFP-CA-Yap and RFP-DN-Yap were further confirmed by heat-shock of animals. Microinjections to generate transgenics were performed at one cell-stage in wild type AB strain zebrafish embryos.

Image quantification

For quantification of Yap intracellular localization, longitudinal sections of individual regenerating blastemas in defined time points stained with anti-Yap and DAPI, were imaged with a Zeiss LSM710 confocal microscope using identical settings (magnification, contrast, gain and exposure time) and XZ projections were made. For each XZ projection, we applied a threshold (8-25 index) in the DAPI channel (visualizing nuclei) to create a binary mask. The DAPI binary mask was superimposed to the anti-Yap channel using the Image Calculator (Multiply option), resulting in the nuclear Yap images. The same approach was followed to obtain cytoplasmic Yap images using the inverse mask. The average intensities of nuclear and cytoplasmic Yap images were determined and normalized to the area. The resultant individual data was processed using Excel, where a ratio of nuclear Yap intensity over cytoplasmic Yap values was calculated for each sample. Total ratios for each condition were plotted using GraphPad Prism software and non-parametric, two-tailed Mann-Whitney tests were performed between the several conditions. For quantification of Yap, F-actin and α-Catenin shifts between proximal and distal locations, longitudinal sections of individual regenerating blastemas in defined time points stained with anti-Yap and phalloidin or anti-GFP (to detect α-Catenin) were imaged as above. For each XZ projection, plot profiles of corresponding intensities were measured, in which maximum intensity values for distal images and minimum intensity values for proximal images were recorded. The resultant individual data was processed using Excel,

where a ratio of proximal over distal values was calculated for each sample. Total ratios were plotted as above.

Proliferation quantifications were performed using an ImageJ plugin, ObjectJ. This plugin was used to manually identify all Geminin and pH3 positive cells and quantify the respective blastema area including the 1st segment proximal to the amputation level. Resultant data was processed and normalized (area normalization) using Excel. Normalized cell divisions (total numbers) were plotted using GraphPad Prism software, and two-tailed Mann-Whitney tests were performed between the several conditions.

For cell density measurements in the blastema, longitudinal sections of individual regenerating blastemas in defined time points counterstained with DAPI to reveal their total nuclei, were imaged with a Zeiss LSM710 confocal microscope using identical settings (magnification, contrast, gain and exposure time). Intensity measurements along blastemas including the 1st segment proximal to the amputation plane were done with the Plot profile tool in ImageJ along rectangular regions of interest (Knopf et al., 2011). The same analysis was performed in intensity quantifications of Phospho-Mst 1/2, Phospho-Lats 1/2 and GFP fluorescence in CA-yap; *ctgfa*:eGFP and DN-yap; *ctgfa*:eGFP transgenics. In the latter case, *in vivo* fluorescent images from individual blastemas of *ctgfa*:eGFP transgenics were acquired using a Zeiss Lumar stereoscope along the full fin including the regenerate.

For intercellular mesenchymal space quantifications in the blastema, longitudinal sections of *ctgfa*:eGFP individual regenerating blastemas in defined time points were analyzed after immunofluorescence with anti-GFP, to reveal the mesenchymal cells morphology and space occupied within the blastema. Imaging was performed in a similar way as above. A threshold (index 35) was applied to the images in order to label all the intercellular mesenchymal space, the LUT was inverted and intensity measurements were performed in a similar way as above. For cell aspect ratio determination, individual mesenchymal cells were manually outlined using ImageJ and measurements to determine values for *x* (major) and *y* (minor) axes of the cells were performed using the Fit Ellipse plugin. Resultant individual data was processed using Excel, where *y* divided by *x* values for each cell were plotted in order to have individual cell aspect

ratios - in which a perfect circular shape corresponds to a ratio between *y* and *x* equal to 1. Total ratios for each condition were plotted using GraphPad Prism software, and two-tailed Mann-Whitney tests were performed between the several conditions. All error bars in graphs correspond to the standard deviation of the mean.

Supplementary Tables

Table S1. Proteins screened through immunohistochemistry in the regenerating blastema. Related to Figs 5 and 6.

Protein	Present in blastema	Stages tested	Cell type labeled	Type of adhesion associated
α-Catenin	Yes	Uncut, 24hpa, 48hpa, 72hpa	Most distal mesenchymal cells; osteoblasts; present in all layers of epidermis *(a)*	Adherens junction
Beta-Catenin	Yes	Uncut, 3hpa, 6hpa, 24hpa, 48hpa, 72hpa	In early stages in the mesenchyme, present in some layers of epidermis, osteoblasts *(a)*	Adherens junction
P120-Catenin	No	72hpa	--	Adherens junction
E-Cadherin	Yes	48hpa, 72hpa	All layers of epidermis	Adherens junction
N-Cadherin	Yes	72hpa	New osteoblasts *(a)*	Adherens junction
M-Cadherin	No	72hpa	--	Adherens junction
P-Cadherin	No	72hpa	--	Adherens junction
R-Cadherin	No	72hpa	--	Adherens junction
Cadherin 5	No	72hpa	--	Adherens junction
Cadherin 11	No	72hpa	--	Adherens junction
Zyxin	No	72hpa	--	Integrin and Actin associated protein
ZO-1	Yes	48hpa, 72hpa	Most apical layer of epidermis, blood vessels	Tight junction
Claudin 1	Yes	72hpa	Most epidermal layers	Tight junction
Fibronectin	Yes	48hpa, 72hpa	Extracellular matrix of all fibroblast-like cells	Extracellular matrix
Laminin	Yes	24hpa, 48hpa, 72hpa	Extracellular space between basal epidermal layer and mesenchyme, blood vessels	Extracellular matrix
Tenascin C	Yes	24hpa, 48hpa, 72hpa	Extracellular space of all mesenchyme *(b)*	Extracellular matrix
F-Actin (Phalloidin)	Yes	Uncut, 6hpa, 24hpa, 48hpa, 72hpa	Initially in epidermis, later restricted to most apical layer of epidermis and all mesenchyme, blood vessels	Cytoskeleton
Phospho-	Yes	Uncut, 6hpa,	Initially in	Cytoskeleton

Myosin Light Chain 2		24hpa, 48hpa, 72hpa	epidermis, later both in epidermis and all mesenchyme, blood vessels	
Phospho-Ezrin/ Radixin/ Moesin (ERM)	Yes	48hpa, 72hpa	Similar to F-actin	Cytoskeleton, Actin associated protein
Scribble	No	72hpa	--	Tight junction
Vinculin	No	72hpa	--	Integrin associated protein

(a) Published in (Stewart et al., 2014), *(b)* Published in (Jaźwińska et al., 2007).

Table S2. Sequences of primers used for cloning and qPCR analysis during this study.

Gene/ Accession no.	Primer sequence		Human/ *Drosophila* orthologue
	Forward Primer (5')	Reverse Primer (3')	
frmd6 / NM_001020816	CCATCGATATGAGCAAACTGACTTTCCACA	CGGGCCCTTACACCACAAACTCTGGTTCTG	*frmd6(willin)/expanded*
nf2b / NM_212951	CGGGCCTGGTTTAACACATA	CAACAGAGCTCGGATTGTTCT	*nf2/merlin*
sav1 / NM_001004560	GTGTCAGTGCCAACCTGGAT	AGTAAGCTGTCTGAGTGTGTCA	*salvador*
stk3 / NM_199672	GCAGTGCTTCCTTAAACTCCAAAC **qPCR:** CCCAGAACAGAGAGCGACGGCAACTCAACT	GCAGGAATCTAGAGTAAGATGCAG **qPCR:** GCCAGCACTCTCGGAACCAGACTTCACCAT	*mst2/hippo*
lats2 / ENSDART00000139620	**qPCR:** GCGTGCCCTGAAACAGACTGGTAGCCGTAA	**qPCR:** GCGTGCCCTGAAACAGACTGGTAGCCGTAA	*lats2/warts*
wwtr1/ NM_001037696	**qPCR:** TGTTACAGCATCCCGACCACTCCTGAAGAC	**qPCR:** CCAGGTGAGGAAGGGCTCGCTCTTGTT	*wwtr1(taz)/n.a.*
yap1 / NM_001139480	CGACTTTCCTTGAAAACGGT **qPCR:** AGCCAAAGTCCCACTCCAGACAAGCCAGTA	AAGGTGTAGTGCTGGGTTCG **qPCR:** GGCAGCGGCATGTCATCAGGTATCTCGTAA	*yap/yki*
tead1a / NM_212847.2	**qPCR:** GCGAACGGGCAAGACACGGACAAGAAAGC	**qPCR:** ACTGTGGATGGCTGTGGCGGAGACAATCTG	*tead1/ scalloped*
tead4 / XM_002666763.3	**qPCR:** AAGGAGGACTGAAGGAGCTGTTCGAGAAGG	**qPCR:** GCCGAATGAGCAGACTTTAGTGGAGGAGGT	*tead4 / scalloped*
ctgfa / NM_001015041	**qPCR:** TCCTCACAGAACCGCCACCTTGCCCAT	**qPCR:** TCACGCCATGTCGCCAACCATCTTCTTGT	*ctgf/n.a.*
ctgfb / NM_001102573	**qPCR:** GAGACAGGCATCTGCATGGCTCAAGAAGGT	**qPCR:** GTCGCACACCCACTCCTCACAGCACTT	*ctgf/n.a.*
amphiregulin / ENSDART00000114293	**qPCR:** ACACTTCCGTGCTGGATCATGTGACTGTGA	**qPCR:** TGGTTCTGCTCGTCTCCTTTACTGGCTTGG	*amphiregulin/ n.a*
fgf20a / NM_001037103	**qPCR:** GGTTCGGTCCAAGGCACGAGG	**qPCR:** CGCTCGCCATGCCGATACAGG	*fgf20/n.a.*
msxB / NM_131260	**qPCR:** CCAGCAGGTCGCGTGTTCTCC	**qPCR:** GCTTGCGTAAGGTGCACGGC	*n.a./drop*
wnt10a / NM_130980	**qPCR:** GCTCTCACGACATCAGTTGGCACTCTCC	**qPCR:** AAGTAATCCATGCTGCTGCTGCTCTTCTGC	*wnt10a/wnt10*
wnt3a / NM_001007185	**qPCR:** GCCCTGATGCCCGCTCTGCTATGAATC	**qPCR:** CCGATGTTTCTCAACCACCATTTCCGATGC	*wnt3a/n.a.*
lef1 / NM_131426	**qPCR:** AAGGCCACCCGTACCCGAGT	**qPCR:** GGGTGAACGGCATGGGACGG	*lef1/pangolin*

dkk1a / NM_001281800	**qPCR:** ACATCCCAGGAGAACCACAG *(a)*	**qPCR:** AAACTTGTCCCTCTGTCAGCA *(a)*	*dkk1/n.a.*
dkk1b / NM_131003	**qPCR:** CTCCGCTCACCCAGGGAATACATCCTACAA	**qPCR:** ACCCGCCGCACCTGAACCGACTTTA	*dkk1/n.a.*
shha / NM_131063	**qPCR:** GGCCAGGGGTTAAGCTGCGT	**qPCR:** CGGCCTTCTGTCCTCCGTCC	*shh/hh*
bmp2a / NM_131359	**qPCR:** CACTCCGTGAACGCAGAGCAGGTTAGCA	**qPCR:** TCGTCTGGGATGGAGGTCAGGTTGAAGAGG	*bmp2/dpp*
bmp2b / NM_131360	**qPCR:** AACCTACAGCCATGACGGTCAAGGCACAG	**qPCR:** CGTTCCAGCCGACATCACTGAAGTCCACAT	*bmp2/dpp*

(a) Published in (Stewart et al., 2014).

Table S3. Details for RNA probes used in the *in situ* hybridization analysis during this study.

Gene	Vector	Sense Probe		Antisense Probe		Hybridization Temperature
		Restriction Enzyme	**Polymerase**	**Restriction Enzyme**	**Polymerase**	
frmd6	pCS2	EcoRV	SP6	BamHI	T3	68ºC
nf2b	pGEM-T-Easy	NcoI	SP6	SpeI	T7	67ºC
sav1	pGEM-T-Easy	NcoI	SP6	SalI	T7	66ºC
stk3	pGEM-T-Easy	ApaI	SP6	SalI	T7	67ºC
yap1	pGEM-T-Easy	SalI	T7	NcoI	SP6	68ºC
ctgfa [(c)]	pSport	BamHI	T7	EcoRI	SP6	67ºC

(c) Published in (Dickmeis et al., 2004).

Table S4. Antibodies used in the immunofluorescence analysis during this study.

Antibody	Host	Dilution	Company
Anti-Yap FL (63.07)	Mouse	1:100	Sta Cruz Biotechnology
Anti-Phospho Mst1(Thr18)/Mst2(Thr180)	Rabbit	1:100	Cell Signalling
Anti-Phospho Lats1 (Thr1079)	Rabbit	1:100	Cell Signalling
Anti-NF2	Rabbit	1:200	Sta Cruz Biotechnology
Anti-GFP	Rabbit	1:200	Invitrogen
Anti_RFP/DsRed	Rabbit	1:100	ABIN
Anti-Beta-Catenin	Mouse	1:200	BD Transduction labs
Anti-E-Cadherin	Mouse	1:200	BD Transduction labs
Anti-N-Cadherin	Mouse	1:100	BD Transduction labs
Anti-R-Cadherin	Mouse	1:100	BD Transduction labs
Anti-P-cadherin	Mouse	1:100	BD Transduction labs
Anti-M-cadherin	Mouse	1:100	BD Transduction labs
Anti-ZO1	Mouse	1:100	Invitrogen
Anti-Claudin1	Rabbit	1:100	Invitrogen
Anti-Fibronectin	Rabbit	1:100	Sigma
Anti-Laminin	Rabbit	1:100	Thermo Scientific
Anti-TenascinC	Rabbit	1:100	US Biological
Anti-Zyxin	Mouse	1:100	Sigma
Anti-Cadherin5	Mouse	1:100	BD Transduction labs
Anti-p120-Catenin	Mouse	1:100	BD Transduction labs
Anti-α-Catenin	Mouse	1:100	BD Transduction labs
Anti-β-Catenin	Mouse	1:100	BD Transduction labs
Anti-Cadherin11	Mouse	1:100	Invitrogen
Anti-Phospho Ezrin (Thr567)/ Radixin (Thr564)/ Moesin (Thr558)	Rabbit	1:100	Cell Signalling
Anti-Phospho Myosin Light Chain 2 (Ser19)	Rabbit	1:100	Cell Signalling
Anti-Scribble	Goat	1:100	Sta Cruz Biotechnology
Anti-Vinculin	Mouse	1:100	Sigma
Anti-Phospho Histone 3	Rabbit	1:400	Millipore
Alexa 488 anti-rabbit	Goat	1:500	Invitrogen
Alexa 488 anti-mouse			
Alexa 568 anti-mouse			
Alexa 633 anti-rabbit			
Alexa 488 anti-goat	Donkey	1:500	Invitrogen